CYCLIC BEHAVIOR OF FRP-WRAPPED COLUMNS UNDER AXIAL AND FLEXURAL LOADINGS

Barbara FERRACUTI and Marco SAVOIA
DISTART – Structural Engineering, University of Bologna, 40136 Bologna, Italy

ABSTRACT

The behavior of r.c. columns wrapped by composite material sheets (FRP) under axial force and cyclic bending is studied. Cyclic constitutive laws for confined and unconfined concrete in compression, for concrete under tension and for steel reinforcing bars are introduced. Numerical results are in good agreement with experimental tests. Hysteretic dissipated energy for cyclic bending is also estimated. Wrapping with FRP is shown to be very effective, increasing significantly ductility of columns under bending.

1 INTRODUCTION

Strengthening by means of FRP wrapping has been proposed since 15 years ago for increasing resistance of r.c. columns subject to high axial loadings. More recently, strengthening for increasing ductility of columns or bridge piers under cyclic flexure received high consideration. FRP-wrapping is now considered a very effective technique for strengthening under seismic actions. Several models exist for FRP-wrapped columns subject to axial compression (*Fib* [1], De Lorenzis [2]). On the contrary, very few studies can be found on columns under axial loading and bending (Chaallal [3]), eventually considering cyclic loading (Sheikh [4]).

In the paper, a fiber model is developed for FRP-wrapped columns under axial loading and cyclic bending. The model is based on cyclic constitutive laws for confined concrete in compression (Mander [5], Spoelstra [6]), for concrete in tension (Yankelevsky [7]) and for steel reinforcement (Zulfiqar [8]). Numerical simulations are in good agreement with experimental results reported in the literature (Sheikh [4]). Hysteresis dissipated energy by cycles at different values of maximum curvature has been also computed. The study confirms that FRP-wrapping is very effective to increase ductility under flexure of r.c. columns.

2 THE PROPOSED MODEL

For a prescribed value of axial force, the corresponding moment – curvature curve is obtained dy dividing the concrete cross-section into a number of layers (called fibers). The assumption of plain strain profile over the column section and perfect bonding between materials is introduced. For a prescribed value of the sectional curvature, a position of neutral axis is chosen, so that the strain profile is assigned. Then, for each fiber (concrete layers and steel bars), cyclic constitutive law is used to obtain the corresponding stress. The correct position of neutral axis is obtained by cheking the resultant of normal stresses over the cross-section be equal (for a given convergence tolerance) to the prescribed value of axial force. Finally, the value of flexural moment is obtained.

The concrete cross – section under compression is subject to confinement due to the presence of FRP-wrapping. For columns under pure compression, usually a confined and an unconfined part of section are considered (*Fib* [1]), depending on the shape of the cross-section and of curvature radius of corners. In the present study, the same distinction between confined and unconfined part of the cross-section as in the purely compressed cross-section is assumed. Then, with reference to the general layer of concrete under axial strain ε, the confined part is assumed to be subject to the same lateral pressure as that of a FRP-wrapped circular cross-section under the

same axial strain ε. This assumption is valid in the case of moderate values of eccentricity of axial load.

2.1 Confined concrete: monotonic loading curve

Mander's model [5] is adopted for confined concrete, where maximum strength (f_{cc}) and corresponding strain (ε_{cc}) are defined as a function of confinement pressure f_l (see Figure 1a):

$$\frac{f_{cc}}{f_{co}} = 2.354 \cdot \sqrt{1 + 7.94 \cdot \frac{f_l}{f_{co}}} - 2 \cdot \frac{f_l}{f_{co}} - 1.254 \ , \qquad \varepsilon_{cc} = \varepsilon_{co} \cdot \left[1 + 5 \cdot \left(\frac{f_{cc}}{f_{co}} - 1 \right) \right]. \tag{1}$$

where f_{co}, ε_{co} are strength and axial strain of unconfined concrete. Constitutive law is then given by

$$\sigma_c = \frac{f_{cc} \cdot (\varepsilon_c / \varepsilon_{cc}) \cdot r}{r - 1 + (\varepsilon_c / \varepsilon_{cc})^r}, \tag{2}$$

where $r = E_c / (E_c - E_0)$, $E_0 = f_{cc} / \varepsilon_{cc}$. For a FRP-wrapped circular cross – section, confinement pressure f_l depends on lateral strain ε_l of reinforcement through an elastic relation:

$$f_l = \frac{2 \cdot t_j}{d_j} \cdot E_j \cdot \varepsilon_l \,, \tag{3}$$

where t_j, d_j, E_j are thickness, diameter and elastic modulus in the circumferential direction of composite. Finally, lateral strain ε_l can be obtained as a function of current axial strain and stress, ε_c and σ_c adopting the damage model proposed in Pantazopoulou [9]:

$$\varepsilon_l = \frac{E_c \cdot \varepsilon_c - \sigma_c}{2 \cdot \beta \cdot \sigma_c}, \tag{4}$$

where $\beta = 5700 / \sqrt{|f_{co}|} - 500\ \beta$. Following Spoelstra [6], an iterative procedure based on eqns (2)-(4) is adopted to obtain the axial stress σ_c for a given value of axial strain ε_c for the confined concrete. Usually, failure is assumed when FRP strain reaches the ultimate strain.

2.2 Hysteretic model for confined and unconfined concrete

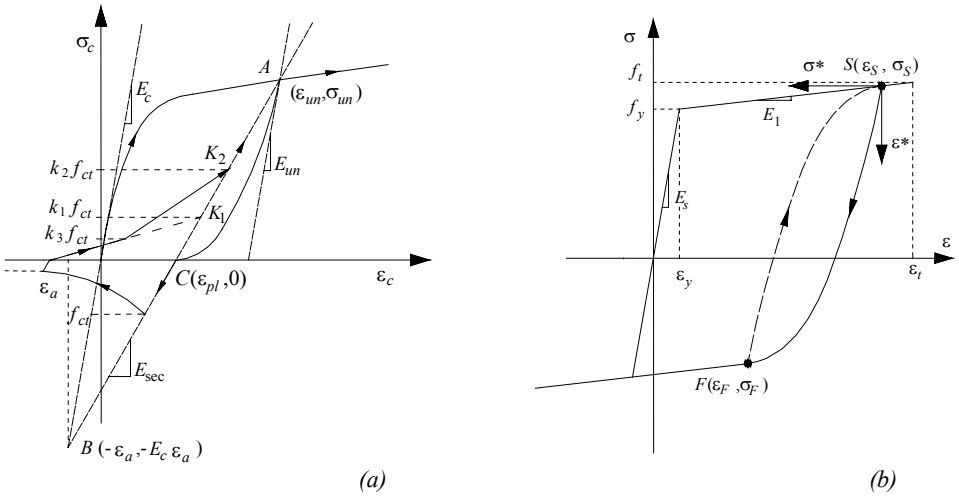

Figure 1: Cyclic behavior of *(a)* confined concrete, *(b)* axial steel reinforcement.

According to Mander model [5], the value of residual plastic deformation ε_{pl} corresponding to complete unloading ($\sigma = 0$) is defined first (see Figure 1*(a)*). That value is obtained as the value for $\sigma = 0$ of the line joining the initial unloading point $A(\varepsilon_{un}, \sigma_{un})$ with point $B(-\varepsilon_a, -E_c \varepsilon_a)$, being E_c the initial elastic modulus and $\varepsilon_a = a\sqrt{\varepsilon_{un}\,\varepsilon_{cc}}$, with $a = \max\left(\varepsilon_{cc}/\varepsilon_{cc} + \varepsilon_{un}, 0.09\,\varepsilon_{un}/\varepsilon_{cc}\right)$, i.e.:

$$\varepsilon_{pl} = \varepsilon_{un} - \frac{(\varepsilon_{un} + \varepsilon_a)\,\sigma_{un}}{(\sigma_{un} + E_c\,\varepsilon_a)}\,. \tag{5}$$

For the unloading curve from $A(\varepsilon_{un}, \sigma_{un})$ to $C(\varepsilon_{pl}, 0)$, Mander proposed an expression analogous to that adopted for monotonic loading:

$$\sigma_c = \sigma_{un} - \frac{\sigma_{un} \cdot x \cdot r'}{r' - 1 + x^{r'}}\,, \tag{6}$$

where $r' = E_{un}/(E_{un} - E_c)$, $x = (\varepsilon_c - \varepsilon_{un})/(\varepsilon_{pl} - \varepsilon_{un})$ and initial unloading modulus is given by $E_{un} = b\,c\,E_c$, where $b = \sigma_{un}/f'_{co} \geq 1$, $c = \left(\varepsilon_{cc}/\varepsilon_{un}\right)^{0.5} \leq 1$. Mander's theory was calibrated for confinement with steel stirrups. Accordingly, unloading curve is independent of confinement pressure. In the case of FRP-wrapping, experimental results show that, for high values of axial loading, unloading curve of confined concrete is almost linear. Hence, the model has been modified by assuming coefficient r' be a function of lateral pressure f_l, so that r' is equal to the one reported above for unconfined case whereas unloading branch is linear for high confinement. Finally, according to plasticity theory, unloading starting from a loading curve is referred to plastic deformation ε_{pl} previously attained.

Cyclic behavior of concrete under tension is modelled starting from Reinhardt model [7]. Concrete behavior under tension is linear for stress lower than tensile strength $f_{ct} = 0.27(f_{co})^{2/3}$, with modulus $E_{\sec} = \sigma_{un}/(\varepsilon_{un} - \varepsilon_{pl})$. The origin of the diagram takes the plastic deformation ε_{pl} previously accumulated into account. Softening branch is then defined by the exponential law:

$$\sigma_c = f_{ct}\left(1 - \frac{\varepsilon_c}{\varepsilon_{ct}}\right)^2\,. \tag{7}$$

For strains greater than $\varepsilon_{ct} = 0.04$ %, residual strength of concrete under traction vanishes.

Loading curves from traction to compression are modified with respect to Reinhardt model, even though the general framework is mantained. Two focus points K_1, K_2 are defined along the line with stiffness E_{sec} with origin in the point (ε_{pl}, 0), corresponding to stress levels $k_1 f_{ct}$ and $k_2 f_{ct}$ (see Figure 1*(a)*). Moreover, $k_3 f_{ct}$ is the tension corrisponding to the transition point between the two branches.

Values adopted for parameters k_1, k_2, k_3 are different from those considered in Reinhardt model. That model was calibrated with reference to experimental results on concrete specimens of small dimensions and without steel reinforcement. In order to calibrate these parameters, some numerical simulations on beams of actual size under flexure are performed and results are compared with experimental data [10]. According to these calibration studies, the values $k_1 = 1$, $k_2 = 4$, $k_3 = 0.5$ have been adopted.

2.3 Hysteretic model for steel reinforcement

For steel bars, Zulfiqar - Filippou model [8] is adopted (see Figure 1*(b)*). A bilinear law is defined for monotonic loading, with elastic modulus E_s, yielding point (ε_y, f_y) and hardening law with modulus $E_1 = (f_t - f_y) / (\varepsilon_t - \varepsilon_y)$, where ($\varepsilon_t$, f_t) defines steel failure.

According to this model, unloading curve starting from point $S(\varepsilon_S, \sigma_S)$ along the hardening branch is given by an exponential law:

$$\sigma^*(\varepsilon^*) = \frac{1 - e^{-\lambda \varepsilon^*}}{1 - e^{-\lambda}}, \tag{8}$$

where $\varepsilon^* = (\varepsilon - \varepsilon_S)/(\varepsilon_F - \varepsilon_S)$ and $\sigma^* = (\sigma - \sigma_S)/(\sigma_F - \sigma_S)$ are normalized strain and stress parameters, so that $(\varepsilon^*, \sigma^*) = (0, 0)$ for $S(\varepsilon_S, \sigma_S)$ and $(\varepsilon^*, \sigma^*) = (1, 1)$ for $F(\varepsilon_F, \sigma_F)$. Moreover, exponent λ is the solution of non linear equation:

$$\frac{\lambda}{1 - e^{-\lambda}} = E_0 \frac{\varepsilon_F - \varepsilon_S}{\sigma_F - \sigma_S}. \tag{9}$$

3 COMPARISON WITH EXPERIMENTAL RESULTS

The proposed model has been validated through comparison with experimental tests by Sheikh and Yau [4] on cyclic behavior of circular columns (diameter 356 mm, 6Φ25 longitudinal steel bars) strengthened by carbon (CFRP) and glass (GFRP) composites, for different values of axial force. Mechanical properties of columns were: f_{co} = 44.8 MPa for specimen ST-4NT and 40.4 MPa for the others; f_y = 450 MPa, f_t = 700 MPa, ε_t = 12%. Properties of FRP-reinforcements are given in Table 1.

Specimen	N/N_u	FRP-wrapping	Thickness (mm)	E_j (MPa)	f_{ju} (MPa)	ε_{ju} (%)
ST-4NT	0.27	CFRP	0.5	75000	900	1.2
ST-5NT	0.27	GFRP	1.25	20000	400	2.0
ST-2NT	0.54	GFRP	1.25	75000	400	2.0
ST-3NT	0.54	CFRP	1.00	20000	900	1.2

Table 1:Properties of different wrapping composites considered in simulations of experimental tests. The value of applied normal force is also reported.

Comparison with experimental tests is reported in Figures 2*(a, b)* for low axial force and in Figures 2*(c, d)* for high axial force. Even though experimental results are not symmetric when moment changes its sign, good agreement can be found between experimental and numerial results.

In particular, unloading and reloading curves are very well reproduced for low axial force, adopting the Mander's unloading curve. On the contrary, for high axial force, good agreement is found if elastic unloading is adopted.

It is worth noting that the behavior of concrete in tension is very important to predict the correct hysteretic behavior of the cross-section. With reference to column ST-4NT, moment – curvature diagram is reported in Figure 3 adopting the proposed law (with $k_1 = 1$, $k_2 = 4$, $k_3 = 0.5$) and neglecting the contribution of concrete in tension (i.e., setting $k_1 = k_2 = k_3 = 0$). Note the excessive pinching effect in the second case when compared with experimental results of Figure 2(*a*), with consequent reduction of dissipated energy in the hysteresis loops.

Finally, for the same tests comparison between experimental and numerically obtained values of hysteretic damping factors are reported in Figures 4. Note that FRP-wrapping provides for a significant increase of ductility under bending. In the unreinforced columns, ductility was about 2 for $N/N_u = 0.27$ and vanishing for $N/N_u = 0.54$. For wrapped columns ductility is about 8 and 5, in the two cases considered. Moreover, the proposed model provides for good results when compared with experimental tests. Predictions adopting Mander's and linear unloading curve are reported.

For low axial loads, the criterion adopted to define unloading curve has a little influence on damping factor; for high axial loads, elastic unloading gives a better prediction of damping factor.

ACKNOWLEDGEMENTS

The financial supports of (italian) MIUR (PRIN 2003 and FIRB 2001 Grants) and C.N.R., PAAS Grant 2001 are gratefully acknowledged.

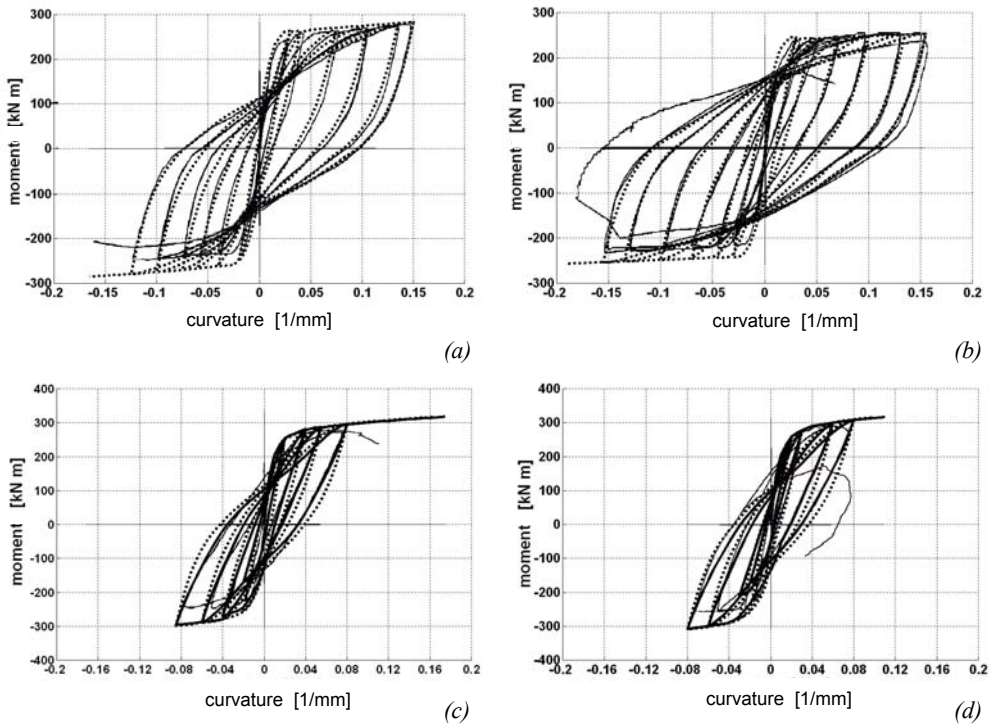

Figure 2: Moment – curvature diagrams for FRP – wrapped column cross-sections under constant axial force and cyclic bending. Experimental results (—) from [4] and numerical results adopting Mander's unloading curve (- - -) or elastic unloading (—): specimens *(a)* ST-4NT, *(b)* ST-5NT, *(c)* ST-2NT, *(d)* ST-3NT.

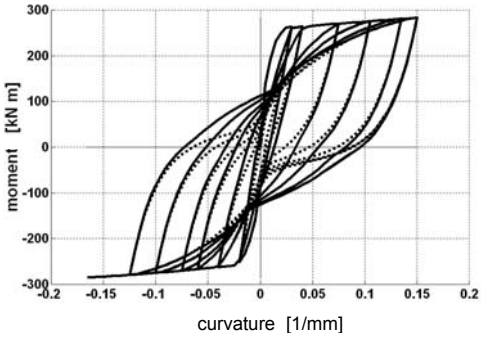

Figure 3: Specimen ST-4NT: Moment – curvature diagram with the proposed model (—) and neglecting the contribution of concrete in tension in reloading branch (- - -).

REFERENCES

[1] FIB, *Externally bonded FRP reinforcement for RC structures*, Fib Bulletin n. 14, 2001.

[2] De Lorenzis, L., Tepfers, R., Comparative study of models on confinement of concrete cylinders with fiber-reinforced polymer composites, *J.Comp.Constr. ASCE*, **7**, 219-237, 2003.

[3] Chaallal, O., Shahawy, M., Performance of fiber-reinforced polymer-wrapped reinforced concrete column under combined axial-flexural loading, *ACI Struct. J.*, **97**, 659-668, 2000.

[4] Sheikh, S.A., Yau, G., Seismic behaviour of concrete columns confined with steel and fiber-reinforced polymers, *ACI Struct J.* **99**, 72-80, 2002.

[5] Mander, J.B., Priestley, M.J.N., Park, R., Theoretical stress-strain model for confined concrete, *J. Struct. Eng. ASCE* **114**(8), 1804-1826, 1988.

[6] Spoelstra, M., Monti, G., FRP-confined concrete model, *J.Comp.Constr.ASCE* **3**, 143-150, 1999.

[7] Yankelevsky, D.Z., Reinhardt, H.W., Uniaxial behavior of concrete in cyclic tension, *J. Struct. Eng. ASCE* **115**(1), 166-182, 1989.

[8] Zulfiqar, N., Filippou, F.C., Models of critical regions in reinforced concrete frames under earthquake excitations, *Report NO. EERC 90-06*, University of California, Berkeley, 1990.

[9] Pantazopoulou, S.J. e Mills, R.H., Microstructural aspects of the mechanical response of plain concrete, *ACI Mat. J.* **92**, 605-616, 1995.

[10] Abrams, D.P., Influence of axial force variation on flexural behaviour of reinforced concrete columns, *ACI Struct. J*, 84, 246-254, 1987.

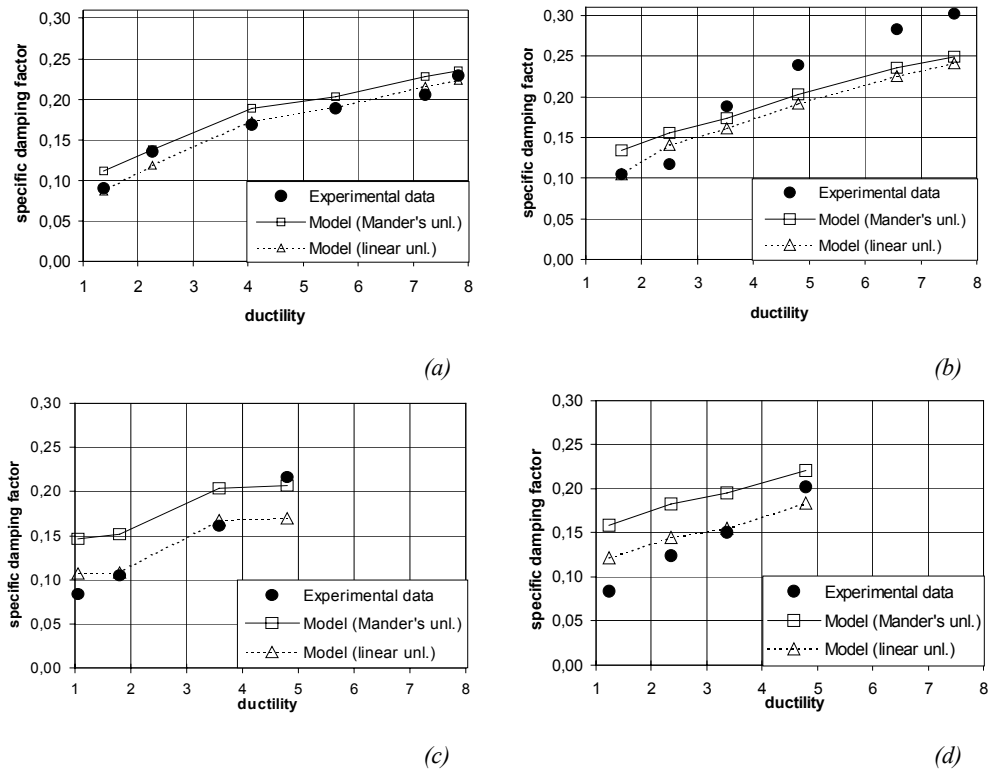

Figure 4: Specific damping ratio vs. ductility: specimens *(a)* ST-4NT, *(b)* ST-5NT, *(c)* ST-2NT, *(d)* ST-3NT.